Plasmodium falciparum is dependent on *de novo myo*-inositol biosynthesis for assembly of GPI glycolipids and infectivity

James I. MacRae[1,4], Sash Lopaticki[2], Alexander G. Maier[2,5] Thusitha Rupasinghe[3], Amsha Nahid[3], Alan F. Cowman[2], Malcolm J. McConville[1,*]

[1]Department of Biochemistry and Molecular Biology, Bio21 Institute of Molecular Science and Biotechnology, 30 Flemington Road, University of Melbourne 3010, Victoria, Australia.

[2]Division of Infection and Immunity, The Walter and Eliza Hall Institute of Medical Research, Parkville 3052, Victoria, Australia.

[3]Metabolomics Australia, Bio21 Institute of Molecular Science and Biotechnology, 30 Flemington Road, University of Melbourne 3010, Victoria, Australia.

[*]Corresponding author: malcolmm@unimelb.edu.au

[4]Current address: The National Institute of Medical Research, The Ridgeway, Mill Hill, London, NW7 1AA, U.K.

[5]Current address: Research School of Biology, The Australian National University, Acton, ACT 0200, Australia.

Running title: Inositol metabolism in *Plasmodium falciparum*

Key words: phospholipid biosynthesis, malaria, glycosylphosphatidylinositol, inositol phosphate

This article has been accepted for publication and undergone full peer review but has not been through the copyediting, typesetting, pagination and proofreading process, which may lead to differences between this version and the Version of Record. Please cite this article as doi: doi/10.1111/mmi.12496

Summary

Intraerythrocytic stages of the malaria parasite, *Plasmodium falciparum*, are thought to be dependent on *de novo* synthesis of phosphatidylinositol, as red blood cells (RBC) lack the capacity to synthesize this phospholipid. The *myo*-inositol headgroup of PI can either be synthesized *de novo* or scavenged from the RBC. An untargeted metabolite profiling of *P. falciparum* infected RBC showed that trophozoite and schizont stages accumulate high levels of *myo*-inositol-3-phosphate, indicating increased *de novo* biosynthesis of *myo*-inositol from glucose-6-phosphate. Metabolic labelling studies with ^{13}C-U-glucose in the presence and absence of exogenous inositol confirmed that *de novo myo*-inositol synthesis occurs in parallel with *myo*-inositol salvage pathways. Unexpectedly, while both endogenous and scavenged *myo*-inositol was used to synthesize bulk PI, only *de novo*-synthesized *myo*-inositol was incorporated into GPI glycolipids. Moreover, gene disruption studies suggested that the INO1 gene, encoding *myo*-inositol 3-phosphate synthase, is essential in asexual parasite stages. Together these findings suggest that *P. falciparum* asexual stages are critically dependent on *de novo myo*-inositol biosynthesis for assembly of a sub-pool of PI species and GPI biosynthesis. These findings highlight unexpected complexity in phospholipid biosynthesis in *P. falciparum* and a lack of redundancy in some nutrient salvage versus endogenous biosynthesis pathways.

Introduction

Malaria remains a major global health challenge, with almost half of the world's population at risk. More than 200 million cases of malaria occur each year resulting in 0.6 million deaths (WHO, 2013, Miller *et al*., 2013). There is no effective, safe anti-malaria vaccine and resistance to frontline drugs is an on-going threat (Dondorp *et al*., 2009). Several species of *Plasmodium* are capable of causing malaria in humans, with *Plasmodium falciparum* being the most important in terms of morbidity and mortality. Disease is associated with the development of asexual stages that undergo repeated cycles of invasion and rapid intracellular replication in red blood cells (RBCs). Infection of RBCs is initiated by the merozoite stage, which subsequently differentiates through several intermediate developmental stages (ring, trophozoite, and schizont) within the parasite-induced parasitophorous vacuole to produce 16-32 new merozoites over a 48 hour period (Boddey and Cowman, 2013). This developmental cycle requires the synthesis of new membrane for production of daughter parasites, as well as the maintenance of the surrounding parasitophorous vacuole and an extensive system of membrane tubules and cisternae in the RBC cytoplasm that are used to export parasite proteins and lipids to the RBC plasma membrane (Besteiro *et al.*, 2010). Additional membrane lipids may also be needed to sustain increased shedding of membrane vesicles from the *P. falciparum*-infected RBC (Mantel *et al.*, 2013; Regev-Rudzki *et al.*, 2013). This demand for new membrane is dependent on the up-regulation of multiple pathways of phospholipid biosynthesis in intraerythrocytic parasite stages as well as the salvage of essential precursors from the host cell (Besteiro *et al.*, 2010). The dissection of these pathways has already led to the development of novel inhibitors that target asexual stages (Ben Mamoun *et al.*, 2010).

Most studies on phospholipid biosynthesis in P. falciparum have focussed on the major phospholipid classes, phosphatidylcholine and phosphatidylethanolamine, and less is know about the synthesis of phosphatidylinositol (PI). While accounting for less than 10% of the total membrane phospholipid (Botté *et al.*, 2013), it fulfils a number of essential functions in intraerythrocytic stages. In addition to contributing to bulk lipid composition of membranes, PI is the precursor for free and protein-linked glycosylphosphatidylinositol (GPI) glycolipids, as well as complex phosphoinositides. Free GPI glycolipids and GPI-anchored proteins dominate the surface of asexual stages (Gerold *et al.*, 1994; Naik *et al.*, 2000; Sanders *et al.*, 2005), have important immuno-modulatory properties and mediate essential host-parasite interactions (Debierre-Grockiego and Schwarz, 2010; Sanders *et al.*, 2005), suggesting that GPI biosynthesis is essential for virulence. PI is also phosphorylated to form phosphoinositides, such as PI-3-phosphate (PI3P) and PI4P, that are proposed to have important roles in regulating protein traffic from the parasite to the RBC membrane, as well as the biogenesis of essential parasite organelles, such as the food vacuole and the apicoplast (Tawk *et al.*, 2010; Tawk *et al.*, 2011; Bhattacharjee *et al.*, 2012b; Bhattacharjee *et al.*, 2012a).

RBC contain very low levels of PI and lack the enzymes needed for the *de novo* synthesis of PI (Allan, 1982), suggesting that intraerythrocytic stages of *P. falciparum* are largely dependent on endogenous PI synthesis (Elabbadi *et al.*, 1994). *De novo* PI synthesis involves the condensation of *myo*-inositol with CDP-diacylglycerol by the membrane-bound enzyme, PI synthase (PIS), located in the ER or other organelles in the secretory pathway (Elabbadi *et al.*, 1994; Wengelnik and Vial, 2007; Michell, 2008). The *myo*-inositol head-group could either be scavenged

from the infected red blood cell or synthesized *de novo* in a two-step pathway involving the initial conversion of glucose 6-phosphate to *myo*-inositol 3-phosphate and the subsequent de-phosphorylation of *myo*-inositol 3-phosphate to *myo*-inositol (Majumder *et al.*, 2003; Fischbach *et al.*, 2006). The *P. falciparum* genome encodes a putative *myo*-inositol synthase (INO1) and two putative inositol-phosphate phosphatases (IMPase), that catalyze the two steps in *de novo* synthesis pathway and all three genes are transcribed in intraerythrocytic stages (Le Roch *et al.*, 2003; Besteiro *et al.*, 2010). On the other hand, infected RBCs and the surrounding serum contain relatively high levels of *myo*-inositol (>200 µM) and exogenous ^{3}H-inositol is incorporated into PI lipids in *P. falciparum* intraerythrocytic asexual stages indicating that salvage pathways are active (Elabbadi *et al.*, 1994). Whether *myo*-inositol salvage and *de novo* synthesis represent parallel or redundant mechanisms for generating *myo*-inositol for PI synthesis remains undefined.

In this study, we have reassessed *myo*-inositol metabolism in these parasites using metabolite profiling, ^{13}C-glucose stable isotope labelling and genetic approaches. We find that *P. falciparum* intra-erythrocytic stages accumulate high levels of inositol 3-phosphate (Ino3P) and that *de novo*-synthesized *myo*-inositol is incorporated into both bulk PI as well as a subcellular pool of PI that is used for GPI glycolipid biosynthesis. In contrast, scavenged *myo*-inositol is primarily used for synthesis of bulk PI. Our findings highlight unanticipated complexity in the inositol metabolism of these parasites and suggest that enzymes involved in *myo*-inositol biosynthesis are novel target of new antimalarial drugs.

Results

Stage-specific differences in inositol metabolism of *P. falciparum*.

Metabolite profiling was used to measure changes in the level of intracellular polar metabolites in *P. falciparum* asexual RBC stages over the 48 hr cycle. Synchronized infected RBC cultures (8% parasitaemia) were sampled at various time points and polar metabolites analysed by GC-MS. Of the 250 metabolite peaks detected, 100 metabolites were identified by reference to authentic standards. The metabolite profiles of unfractionated cultures containing infected (iRBC) and uninfected (uRBC) RBC, clearly changed during the development of intracellular parasite stages through ring, trophozoite and schizont stages, as shown by multivariate principal component analysis (PCA) analysis (Fig 1A). These cultures were also clearly distinguished from RBCs that had never been exposed to *P. falciparum* (nRBC in Figure 1A). To further identify metabolite changes associated with parasite development, polar metabolite levels in trophozoite- and schizont-infected RBC and corresponding uninfected RBC isolated from the same culture were quantitated by GC-MS (Figure 1B). All stages were again clearly separated from each other (Figure 1B), indicating marked changes in metabolite levels of different late asexual stages. Univariate analysis of uRBCs and iRBCs from trophozoite- (Figure 1C) and schizont- (Figure 1D) enriched cultures identified a number of metabolites that were significantly up-regulated during infection. Consistent with a number of recent studies (Teng *et al.*, 2009; Olszewski *et al.*, 2009; Macrae *et al.*, 2013; Sana *et al.*, 2013), the steady-state concentrations of intermediates in glycolysis (e.g. fructose 6-phosphate, α-glycerophosphate, and phosphoenolpyruvate), the pentose phosphate pathway (e.g. ribose 5-phosphate and *sedo*-heptulose 7-phosphate), and the TCA cycle (e.g. succinate, fumarate, and malate) were all increased in iRBCs (Figure 1C, D). As shown recently, the

mitochondrial catabolism of glutamine in the TCA may require transaminase reactions involving the non-proteinogenic amino acid γ-aminobutyric acid, which was present at elevated levels in trophozoite/schizont-infected RBC (Fig 1C,D).

Unexpectedly, levels of Ino3P, a putative intermediate in the pathway of *de novo myo*-inositol biosynthesis, were also highly elevated in iRBC (Figure 1C, D). Ino3P was present at <10 nmol/10^8 nRBCs and ring-iRBCs, but increased to 380 and 450 nmol/10^8 parasitized cells in trophozoite- and schizont-iRBCs, respectively (Figure 2). Increased Ino3P levels was only observed in iRBCs, and not in uRBCs isolated from the same culture or in nRBC (Figure 2). In contrast, both iRBCs and uRBCs isolated from the same culture contained similar levels of non-phosphorylated *myo*-inositol (Fig 2). The levels of *myo*-inositol in iRBC and uRBC were substantially higher than in RBC that had never been exposed to *P. falciparum* (Fig 2). As RBC lack the enzymes needed for *de novo myo*-inositol synthesis, these results suggest that factors secreted or released from iRBC can lead to increased uptake of *myo*-inositol by uninfected RBC in the same culture.

De novo myo-inositol biosynthesis is up-regulated in _P. falciparum_-infected RBCs at mid- and late-stages of infection.

Ino3P can be synthesized from Glc6P, the canonical pathway of *de novo myo*-inositol biosynthesis (Figure 3A), or by direct phosphorylation of *myo*-inositol (Stephens *et al.*, 1990; Shi *et al.*, 2005). To distinguish between these possibilities, synchronized *P. falciparum*-iRBCs containing ring, trophozoite or schizont stages were pulse-labelled with ^{13}C-U-glucose (6 mM) for 2 hr and the incorporation of ^{13}C into intermediates in the *de novo myo*-inositol pathway (Glc6P, Ino3P and *myo*-inositol) quantified by GC-

MS (Figure 3B, Table S1). The rate of turnover of Glc6P, Ino3P and *myo*-inositol increased progressively as parasites developed from ring to trophozoite and schizont stages (Fig 3B). Significantly, the level of ^{13}C-enrichment in Ino3P in trophozoite/schizont stages was comparable to that of Glc6P indicating that Ino3P is primarily or exclusively synthesized from glucose 6-phosphate (Figure 3B, Table S1). In contrast, levels of enrichment in *myo*-inositol were approximately 20-40% of that found in Ino3P. These data suggest that *de novo* synthesis of Ino3P and *myo*-inositol is substantially up-regulated in trophozoite/schizont stages, but that approximately 60% of cellular *myo*-inositol is derived from exogenous sources under these growth conditions.

Transcription of the INO1 gene, encoding the single Ino3P synthase, is increased in *P. falciparum* trophozoite and schizont asexual stages (Bozdech *et al.*, 2003). To determine whether INO1 activity is indeed up-regulated in these stages, cell-free extracts of ring, trophozoite- and schizont-infected RBC were incubated with ^{13}C-glucose 6-phosphate and conversion to ^{13}C-Ino3P measured at various time points over 4 hours by GC-MS. Consistent with the *in vivo* labelling studies, RBC cultures enriched for ring stages contained very low levels of INO1 activity, while INO1 activity was highly elevated in RBC containing trophozoite and schizont stages (Figure 3C). Uninfected RBCs had no measurable INO1 activity (Figure 3C).

The level of ^{13}C-enrichment in *myo*-inositol was always lower than in Ino3P, likely reflecting the uptake of unlabelled *myo*-inositol, which is present at 0.2 mM in RPMI medium. To investigate whether the *de novo* synthesis of *myo*-inositol is repressed when exogenous supplies of *myo*-inositol are increased, trophozoite-iRBCs were

labelled with ^{13}C-U-glucose in the presence of 0.2 mM or 4 mM *myo*-inositol. Incubation in the presence of 4 mM *myo*-inositol led to a 7-fold increase in intracellular levels of *myo*-inositol and a concomitant decrease in ^{13}C-enrichment in this pool (Figure 3D). In marked contrast, increased levels of exogenous *myo*-inositol had no effect on either the abundance of Ino3P or its metabolic labelling with ^{13}C-glucose (Figure 3D). Collectively, these data show that *de novo* synthesis of Ino3P is highly up-regulated in trophozoite and schizont stages and that flux into this pathway is not repressed by exogenous inositol, even when the uptake of exogenous *myo*-inositol is increased.

De novo-synthesized and salvaged _myo_-inositol are used to synthesize PI, but only _de novo_ synthesized _myo_-inositol is incorporated into GPIs.

The up-regulation of *de novo myo*-inositol biosynthesis in trophozoite and schizont stages likely reflects a requirement for bulk membrane phospholipids, as well as the synthesis of phosphoinositides and GPI glycolipids. PI levels increased 2-fold in ring-iRBCs compared to background (non-infected RBCs) and by ~7-fold in trophozoite- and schizont-iRBCs as determined by GC-MS of unfractionated RBC cultures (Figure 4A) and LC-MS analysis of total lipids of non-infected and trophozoite-iRBCs (Table S2). Nineteen different PI molecular species, containing fatty acids of different length and degree of saturation were detected in the LC-MS analyses (Table S3, Figure S1). To investigate whether the *de novo*-synthesized or scavenged *myo*-inositol was used to synthesize bulk PI, trophozoite-iRBCs were labelled with ^{13}C-U-glucose and incorporation of ^{13}C-inositol into PI was monitored by LC-MS (Figure 4B, Table S3). Precursor ion scanning for PI molecular species containing unlabelled or labelled *myo*-inositol head-groups (loss of m/z 241 or 247, respectively) indicated that both

scavenged and *de novo* synthesized *myo*-inositol was incorporated into major PI species (Figure 4B, lower two panels). Additional PI isotopomers (containing 3 or 9 ^{13}C atoms) were also detected, corresponding to molecular species with a labelled glycerol backbone (Figure 4B). Significantly, PI molecular species containing labelled fatty acid components were not detected (data not shown), consistent with asexual RBC stages having minimal *de novo* fatty acid biosynthesis (Tarun *et al.*, 2009). No labelling of either the inositol or glycerol backbone PI pools in non-infected RBC were detected, consistent with the absence of active PI synthesis in these host cells (data not shown).

To investigate whether the source of *myo*-inositol used for PI synthesis is regulated by the availability of exogenous sources, trophozoite-infected RBCs were labelled with ^{13}C-glucose in the presence or absence of 4 mM *myo*-inositol. ^{13}C-enrichment in PI was greatly reduced in the presence of exogenous *myo*-inositol (Figure 4C), confirming that exogenous *myo*-inositol can displace the need for endogenous Ino3P/*myo*-inositol for bulk PI synthesis. The incorporation of exogenous *myo*-inositol into PI was further confirmed by metabolic labelling of trophozoite-iRBCs with ^{3}H-*myo*-inositol. Label was incorporated exclusively into a lipid species that co-migrated with authentic PI and was sensitive to PI-specific phospholipase C but not GPI-specific phospholipase D (Fig 5A), consistent with the known-specificities of these two lipases. Unexpectedly, these experiments showed that exogenous ^{3}H-*myo*-inositol was not detectably incorporated into GPI precursors (Fig 5A). In contrast, in parallel labelling studies, ^{3}H-glucosamine, a component of the conserved glycan core of GPI glycolipids, was rapidly incorporated into the expected intermediates, indicating that GPI biosynthesis was active under these conditions (Fig 5A). To

investigate whether GPI glycolipids are assembled on PI species containing *de novo*-synthesized *myo*-inositol, trophozoite-iRBCs were metabolically labelled with ^{13}C-U-glucose for 2 hr and the glycan head-groups of purified GPIs were analysed by GC-MS. Comparable levels of ^{13}C-enrichment were observed in both the *myo*-inositol moiety and the mannose residues of the glycan backbone of free GPI glycolipids (Figure 5B). These results show that GPI glycolipids are selectively assembled on a sub-pool of PI species that contain *de novo*-synthesized, rather than salvaged *myo*-inositol.

***P. falciparum INO1* is likely to be essential for intracellular development.**

Our data suggested that *de novo myo*-inositol biosynthesis may be specifically required for synthesis of PI pools destined for GPI biosynthesis. To investigate whether this *de novo* biosynthetic pathway is essential, we attempted to disrupt the *P. falciparum* PF3D7_0511800, encoding INO1 in the presence of exogenous *myo*-inositol. All attempts to insert a non-functional gene cassette into the *INO1* locus were unsuccessful (Figure 6). In contrast, insertion of a HA/STREP-tag into the locus was successful (Figure 6) indicating that it is possible to target this locus. These results provide strong evidence that INO1 provides an essential pool of *myo*-inositol and PI that cannot be by-passed by the presence of exogenous inositol.

Discussion

RBC lack the capacity to synthesize PI and intraerythrocytic stages of *P. falciparum* are predicted to be dependent on *de novo* PI synthesis for survival within this niche. In this study, we show that asexual parasite stages utilize *myo*-inositol that has been scavenged from the host as well as endogenously synthesized *myo*-inositol for the

synthesis of bulk membrane PI. However, only *de novo*-synthesized *myo*-inositol is incorporated into a sub-pool of PI species that are used for GPI biosynthesis in the ER. These analyses indicate that the pathway of *de novo* synthesis of *myo*-inositol, which is highly up-regulated in asexual stages, cannot be by-passed by *myo*-inositol salvage pathways and is critical for the assembly of essential surface glycolipids and GPI-anchored proteins.

The up-regulation of Ino3P synthesis in trophozoite and schizont stages was initially detected in an untargeted metabolomic analysis of unfractionated and purified infected RBC. These analyses revealed a dramatic increase in the intracellular concentration of Ino3P in infected RBC cells. The accumulation of Ino3P has also recently been reported in asynchronized *P. falciparum* RBC stages (Sana *et al.*, 2013). *In vivo* and *in vitro* ^{13}C-glucose labelling studies demonstrated that Ino3P was synthesized from glucose 6-phosphate, rather than the phosphorylation of exogenous *myo*-inositol, and subsequently dephosphorylated to form *myo*-inositol, reflecting operation of the canonical pathway of *myo*-inositol biosynthesis. *De novo* synthesized *myo*-inositol was incorporated into both bulk PI as well as newly synthesized GPI glycolipids. In contrast, exogenous *myo*-inositol was only incorporated into bulk PI. The latter conclusion was supported by the findings that (1) exogenous ^{3}H-*myo*-inositol was incorporated into bulk PI but not GPI in short term labelling studies, (2) addition of exogenous *myo*-inositol to *P. falciparum* RBC cultures reduced the extent to which endogenous Ino3P was incorporated into bulk PI, but had no effect on incorporation into the GPI pool, and (3) comparable levels of ^{13}C-enrichment occur in the *myo*-inositol and mannose residues of GPI head-groups in ^{13}C-glucose-fed parasites, indicating that newly synthesized GPIs contain predominantly or

exclusively *de novo*-synthesized *myo*-inositol. Collectively, these results suggest that synthesis of endogenous Ino3P is required to sustain levels of PI in the endoplasmic reticulum that are used for GPI biosynthesis, providing an explanation for the apparent essentiality of the INO1 gene in the presence of robust *myo*-inositol salvage pathway.

Related findings have been made in the insect and mammalian-infective stages of *Trypanosoma brucei*, the causative agent of human African trypanosomiasis (HAT) or Nagana in cattle. RNAi-mediated down-regulation of either INO1 or the single H^+-inositol transporter in these parasites resulted in loss of viability or reduced growth, respectively (Martin and Smith, 2006b; Martin and Smith, 2006a; Gonzalez-Salgado *et al.*, 2012). Reminiscent of the situation in *P. falciparum*, repression of INO1 expression in *T. brucei* bloodstream stages had little effect on synthesis of bulk PI but resulted in reduced synthesis of GPI precursors (Martin and Smith, 2006b; Martin and Smith, 2006a). Conversely, repression of inositol transporter expression had little effect on GPI biosynthesis but resulted in reduced bulk PI synthesis (Gonzalez-Salgado *et al.*, 2012). In *T. brucei*, a single isoform of PI synthase is compartmentalized to the ER and Golgi, and an H^+/inositol transporter is targeted to the Golgi apparatus as well as the plasma membrane (Gonzalez-Salgado *et al.*, 2012; Martin and Smith, 2006b). Based on the localization of these enzymes and transporters, it has been proposed that cytoplasmic pools of *myo*-inositol, comprising both scavenged and endogenous *myo*-inositol are transported into the lumen of the Golgi and used by the Golgi PI synthase to make bulk PI and related lipids (Gonzalez-Salgado *et al.*, 2012; Martin and Smith, 2006a). In contrast, the ER-located PI synthase, which may be orientated with catalytic domain on the cytosolic (Fischl *et*

al., 1986) or luminal face of the ER, is proposed to only have access to *de novo*-synthesized *myo*-inositol. Key elements of this model remain to be defined, including the precise topology of the ER/Golgi PI synthases and the mechanism by which *de novo*-synthesized *myo*-inositol is channelled to the ER isoform of PI synthase.

The compartmentalization of inositol and PI synthesis may be achieved in different ways in *T. brucei* and *P. falciparum*. In particular, *P. falciparum* encodes for only one isoform of PIS (PF3D7_1315600), suggesting that this enzyme has a dual location or that different pools of PI are synthesized within the ER. The presence of a single isoform of PIS also indicates a common membrane topology for all PI synthetic reactions. While there is little information on the topological orientation of PI synthases in other organisms *in vivo* (Fischl *et al.,* 1986), the presence of *myo*-inositol membrane transporters in the Golgi membranes of *T. brucei* and the Golgi/ER membrane of humans cells, supports a luminal sidedness for this reaction (Gonzalez-Salgado *et al.*, 2012; Di Daniel *et al.*, 2009). Conversely, while *T. brucei* expresses a single isoform of the inositol-phosphate phosphatase (IMPase), that catalyzes the second step in the INO1 pathway of *myo*-inositol synthesis, *P. falciparum* expresses two IMPases. These proteins contain conserved synaptojanin-like IMPase domains and are predicted to be targeted to the cytoplasm (PF3D7_0705500) or intracellular membranes (PF3D7_0802500), respectively. Cytosolic and membrane-bound forms of IMPase are also predicted to occur in other organisms (Vadnal *et al.,* 1992; Miller and Allemann, 2007). Whether these proteins have redundant functions in *myo*-inositol synthesis or are involved in channelling different pools of *myo*-inositol to the ER or Golgi-located PI synthase remains to be determined. However, the fact that only one IMPase is required for metabolic compartmentalization in *T. brucei* implies

that the two *P. falciparum* IMPases also have a common cytoplasmic topology. Taken together, we propose a revised model in which Ino3P is selectively channelled to the ER PIS via an IMPase/*myo*-inositol transporter (Figure 7). PI generated in the ER is subsequently flipped to the cytoplasmic face where it is utilized by the initial enzymes in GPI biosynthesis that utilize the sugar donor UDP-GlcNac and have catalytic domains orientated on the cytoplasmic side of the ER (Chang *et al.*, 2002). However, further work is needed to determine the localisation of *myo*-inositol transporters and IMPase isoforms and validate this model.

Interestingly, there is evidence that ER pools of PI are also phosphorylated to generate a functionally important sub-pool of PI3P in apicomplexan parasites (Tawk *et al.*, 2011). In both *Plasmodium* spp. and *Toxoplasma gondii*, PI3P has been localized to the cytoplasmic face of ER-derived membrane vesicles and shown to be required for apicoplast biogenesis (Tawk *et al.*, 2010; Tawk *et al.*, 2011). PI3P is also proposed to accumulate in the lumen of the ER in *Plasmodium* RBC stages where it might be involved in regulating the export of secretory proteins (Bhattacharjee *et al.*, 2012a; Bhattacharjee *et al.*, 2012b). However, other models have been proposed (Rommisch, 2012) and the extent to which PI3P is transported into the lumen of ER remains to be determined.

Our findings highlight significant differences in inositol metabolism in different eukaryotic pathogens (Reynolds, 2009). In common with *P. falciparum* asexual stages, a number of other protozoan and fungal pathogens, such as *Leishmania mexicana* (Ilg, 2002) and *Candida albicans* (Chen *et al.*, 2008) can generate all of their *myo*-inositol requirements via the INO1 dependent pathway and proliferate

normally in the absence of exogenous *myo*-inositol. *Cryptococcus neoformans* is also prototrophic with regard to *myo*-inositol. However, this fungal pathogen can also catabolize *myo*-inositol as a major carbon sources and is dependent on *myo*-inositol uptake for survival in *myo*-inositol-rich niches, such as the brain, within its animal host (Xue *et al.*, 2010; Wang *et al.*, 2011). In contrast, *T. brucei* procyclic forms cannot survive without an exogenous supply of *myo*-inositol, despite having a functional INO1-dependent pathway (Gonzalez-Salgado *et al.*, 2012). It is possible that *myo*-inositol uptake in *T. brucei* procyclic forms is required to spare endogenous Ino3P for ER-directed PI biosynthesis and production of GPI anchor precursors that in turn are needed for expression of the dominant variant surface glycoprotein. On the other hand, the apicomplexan parasite, *Toxoplasma gondii*, lacks an annotated INO1 gene and is predicted to be completely dependent on exogenous *myo*-inositol for inositol-lipid synthesis. How *T. gondii* regulates the synthesis of different pools of PI needed for bulk lipid and GPI biosynthesis remains to be determined.

INO1 is commonly considered to be the rate-limiting step in *de novo myo*-inositol biosynthesis. However, in *P. falciparum*, the down-stream IMPases, rather than INO1, appear to be rate-limiting as shown by the rapid labelling and accumulation of Ino3P in ^{13}C-glucose-fed parasites and the comparatively slow chase of ^{13}C- into free *myo*-inositol. The accumulation of Ino3P in late RBC parasite stages was striking and may be needed to sustain a high flux into the essential ER pathway of PI synthesis (Fig 6). Alternatively the accumulated Ino3P pool may constitute an internal ‘reserve’ of *myo*-inositol which can be used to maintain inositol-lipid biosynthesis under conditions when either exogenous inositol or glucose are limiting. Unlike non-phosphorylated *myo*-inositol, Ino3P is effectively trapped within the parasites and not susceptible to

reverse transport by diffusion-driven plasma membrane facilitative transporters. Ino3P could also have additional roles, independent of inositol-lipid biosynthesis. In particular, Ino3P synthesis is closely coupled to the formation of glucose 6-phosphate, and the size of the Ino3P pool could reflect nutrient availability and the energy status of asexual stages. Ino3P could also be converted to more complex inositol polyphosphates (Stritzke *et al.*, 2012) which have been shown to regulate multiple cellular processes in other eukaryotes, including cell signalling, cell cycle control, host cell invasion and parasite maturation (Irvine and Schell, 2001; Luo *et al.*, 2011). Finally, there is accumulating evidence that the *P. falciparum* INO1 pathway and PI synthesis might be primarily regulated at the post-transcriptional level. In particular, enzymes involved in PI metabolism were highly enriched in the *P. falciparum* schizont phosphoproteome (Lasonder *et al.*, 2012). Similarly, the yeast INO1 enzyme has also recently been shown to be regulated by phosphorylation (Deranieh *et al.*, 2013). Collectively, these findings suggest that inositol metabolism and lipid biosynthesis is highly regulated both at the level of enzyme activity and subcellular compartmentalization. The dependence of *P. falciparum* asexual stages on the INO1 pathway makes these regulatory mechanisms attractive targets for new drugs.

Experimental Procedures

Cell culture. *Plasmodium falciparum* 3D7 parasites were cultured in 4% haematocrit with RPMI 1640 and glucose-free RPMI media (both Sigma) as appropriate, supplemented with hypoxanthine (52 mg/L, Calbiochem), 0.5% AlbuMAX (Gibco), sodium hydrogen carbonate (0.21%, BDH), and gentamycin (0.58 mg/L, Pfizer), as described previously (Trager and Jensen, 1976). Parasite synchronization was achieved by repeated sorbitol lysis (Lambros and Vanderberg, 1979). Infection was

assessed by light microscopy. Human blood was kindly donated by the Red Cross Blood Service (Melbourne, Australia).

Saponin lysis of RBC membranes. *P. falciparum* infected RBCs were harvested by centrifugation (1500 rpm, 5 min, room temperature) and the cell pellet resuspended in 0.15% saponin (Kodak) in PBS (10 min, on ice) before washing twice in cold PBS (pH 7.4). Cell preparations were freeze-thawed before use.

Metabolite extraction of *P. falciparum*-infected and uninfected RBCs. *P. falciparum*-infected/uninfected RBC cultures (~ 8% parasitaemia) were centrifuged (1500 rpm, 10 min, room temperature) and the cell pellet resuspended in fresh medium which was subsequently rapidly chilled to 0^{o}C by immersion of the tube in a dry ice/ethanol slurry (Saunders *et al.*, 2011; Macrae *et al.*, 2012). In some experiments, mature trophozoite- or schizont-infected RBCs were purified from uninfected and ring stage trophozoite-infected RBCs by magnet purification (see below). The chilled RBCs (10^8) were harvested by centrifugation (1500 rpm, 10 min, 0 °C), washed three times with ice cold PBS (pH 7.4) and extracted in chloroform/ methanol/water (1:3:1 v/v/), containing *scyllo*-inositol (1 nmol) as internal standard (60 °C, 20 min). Polar and apolar metabolites were separated by phase partitioning (Saunders *et al.*, 2011).

Polar metabolite extracts were methoximated and trimethylsilyl (TMS) derivitized, prior to analysis by GC-MS (Saunders *et al.*, 2011). Apolar metabolite extracts were subjected to methanolysis prior to TMS derivitization and analysis by GC-MS (McConville *et al.*, 1990). GC-MS was performed with a Hewlett-Packard 6890-5973

system. Derivitized samples were infected onto a DB-5MS + DG column (30m × 0.25 mm, with 10m inert gap, J&W, Agilent Technologies) in splitless mode (injection temperature 270 °C for methoximation-derived samples and 280 °C for methanolysis-derived samples) using helium as the carrier gas. For methoximated polar metabolite analyses, the initial oven temperature was 70 °C (2 min), followed by temperature gradients to 295 °C at 12.5 °C/min, and from 295 °C to 320 °C at 25 °C/min. The final temperature was held for 3 min. For analysis of fatty acid methyl esters, the initial oven temperature was 80 °C (2 min), followed by temperature gradients to 140 °C at 30 °C/min, from 140 °C to 250 °C at 5 °C/min, and from 250 °C to 265 °C at 15 °C/min. The final temperature was held for 10 min. Data analysis was performed using Chemstation software (MSD Chemstation D.01.02.16, Agilent Technologies). Metabolites were identified by comparison of retention times and ion fragmentation patterns with authentic standards. Quantification of metabolites was calculated using the formula: amount metabolite (nmol) = (area metabolite(s)/area *scyllo*-inositol) × (1 nmol *scyllo*-inositol /$^{metabolite}MRRF_{sI}$); where $^{metabolite}MRRF_{sI}$ is the molar relative response factor determined from the mean value of: area appropriate metabolite peak/area *scyllo*-inositol peak (1:1 standards).

Magnet-purification of trophozoite- and schizont-stage *P. falciparum*-infected RBCs. *P. falciparum*-infected/uninfected cell cultures were centrifuged, resuspended in fresh medium and metabolically quenched, as described above. Mature trophozoite- and schizont-infected RBCs were purified from uninfected and ring-stage infected RBCs by passage through a CS Column on a VarioMACS magnetic cell separator (Miltenyi Biotec) at 4°C as described previously (Trang *et al.*, 2004). Mature

trophozoite- and schizont-infected RBCs were eluted with 1/5 culture volume of ice-cold medium.

Stable isotope labelling of *P. falciparum*-infected RBCs. *P. falciparum* RBC cultures were synchronized by repeated sorbitol lysis (Lambros and Vanderberg, 1979) and suspended in fresh RPMI medium containing 6 mM ^{13}C-U-glucose (Spectra Stable Isotopes). After incubation for 2 hr, cultures were harvested and metabolites extracted as above. Parallel incubations and extractions were performed on uninfected RBCs. ^{13}C-enrichment in different polar metabolites was quantified by GC-MS analysis as previously described (Saunders *et al.*, 2011), and fractional enrichment based on the calculated ratio of ^{12}C-/^{13}C-glucose in the medium. In some experiments, the RPMI medium (containing 0.2 mM *myo*-inositol) was supplemented with an additional 4 mM *myo*-inositol.

Statistical analyses.

GC-MS chromatograms (n = 5-8 for any given sample) were processed with AnalyzerPro (SpectralWorks) or PyMS (http://code.google.com/p/pyms/). Data were normalized by centering samples using the median values and scaled by inter-quartile range (IQR). Missing values were imputed as half of the minimum abundance detected in other groups. PCAs were generated using Simca-P 11 software (Umetrics) while Z-transformation (using PyMS) was performed in order to scale each metabolite in the infected-RCS according to its corresponding value in the uninfected-RBC. Box-whisker plots were generated using R statistics software (www.R-project.org).

PI quantification. Synchronised *P. falciparum*-infected RBCs (at ~17 % parasitaemia) enriched for ring, trophozoite and schizont stages, and non-infected RBCs were metabolically quenched and harvested as described above. RBC (2×10^8) were extracted in chloroform/methanol/water (1:3:1 v/v/v), centrifuged to remove insoluble material and the supernatant dried under nitrogen and phase partitioned in butan-1-ol/water (200 µL:200µL). An internal standard of 1 nmol *scyllo*-inositol (*s*I) was added to the PI-containing apolar phase and subsequently dried, methoximated and analysed by GC-MS as described above.

Measurement of *in vitro* INO1 activity. A two stage assay was developed in which ^{13}C-glucose was quantitatively converted to ^{13}C-glucose 6-phosphate with purified hexose kinase, and then incubated with *P. falciparum* lysates to generate Ino3P. The conversion of ^{13}C-glucose to ^{13}C-glucose 6-phosphate was achieved by incubating 300 µM ^{13}C-U-Glc with hexokinase (66 µg/mL, Sigma) in assay buffer (1 mM ATP (Sigma), 2.5 mM $MgCl_2$ (BDH, AnalaR), 100 mM TrisHCl (pH 7.5, Sigma), 14 mM NH_4Cl (Ajax), 0.8 mM NAD^+ (Sigma)) at 37 °C for 10 min and the hexose kinase denatured by boiling for 10 min. *P. falciparum* lysates were prepared by suspending unfractionated infected RBCs or non-infected RBCs in ice-cold lysis buffer (1 mM NaHEPES (pH 7.4, Sigma), 2 mM ethylene glycol tetraacetic acid (Sigma), 2 mM dithiothreitol (Biovectra)) for 10 min. Aliquots (50µL) of ^{13}C-glucose 6-phosphate and cell lysate (5 x10^7 RBC equivalents (~5 x 10^6 infected RBC)) were incubated at 37 °C and the reactions stopped after 0, 0.5, 1, 5, 10, 30, 60, 120, 180, and 240 by boiling for 5 min. Polar products were recovered after extraction of the mixture in chloroform/ methanol/water (1:3:3 v/v/v, containing 1 nmol *scyllo*-inositol), and the synthesis of ^{13}C-Ino3P quantified by GC-MS.

Extraction, purification and analysis of radiolabelled GPI anchor intermediates. Synchronized *P. falciparum* RBC cultures were metabolically labelled with ^{3}H-*myo*-inositol or ^{3}H-glucosamine [2.5 μCi/mL], starting at 12hr in the 48 hr asexual cycle. Infected RBC were harvested after 24 hr (late trophozoite stage) by magnet purification and GPI glycolipids extracted as described previously (McConville and Blackwell, 1991). Briefly, cell pellets were lyophilized and lipids were extracted twice in chloroform/methanol/water (1:2:0.8, v/v) for >1 hr at room temperature. Combined supernatants were dried under nitrogen and glycolipids recovered after 1-butanol/water (2:1 v/v) phase partitioning. The 1-butanol phases were dried and analysed by high performance thin layer chromatography (HPTLC) on Silica Gel 60 plates (Merck) developed in chloroform/methanol/13 M ammonia/1 M ammonium acetate/water (180:140:9:9:2.3 v/v). Radioactive species were visualised by fluorography after spraying with EN^{3}HANCE (PerkinElmer Life Sciences) and the major GPI species identified from their HPTLC migration, as reported previously (Gerold *et al.*, 1994).

Enzyme digestions. Radiolabelled lipids were incubated with PI-PLC (146 mU, ICN) in 25 mM triethanolamine (pH 7.4), 5 mM ethylenediaminetetraacetic acid, 0.08% Triton X-100 (Sigma) or with rabbit serum (2 μL, a source of serum GPI-PLD) in 50 mM Tris-HCl (pH 7.4), 10 mM sodium chloride, 2.6 mM calcium chloride, 0.1% Nonidet P40 (ICN), at 37 °C for 16 hr. For the GPI-PLD digests, additional 2 μL aliquots of rabbit serum were added after 1 hr and 2 hr. The digests were phase partitioned in butan-1-ol/water (1:1, v/v) and the apolar phase dried under nitrogen for HPTLC analysis.

Analysis of GPI glycolipids. Synchronized *P. falciparum* RBC cultures were metabolically labelled with ^{13}C-glucose (26 hr), and infected RBC containing late trophozoite stages were isolated by magnet separation. Total lipid was extracted in chloroform/methanol/water (1:2:0.8, v/v) and recovered in the organic phase after butan-1-ol/water partitioning. Lipid (2×10^8 cell equivalents) were dried under nitrogen, resuspended in 10% propan-1-ol/100 mM NH_4Ac and loaded onto a column of octyl-Sepharose (50 mm × 11 mm) equilibrated in the same buffer. Phospholipids (containing two acyl-chains) and resolved from later eluting GPI glycolipids (containing three acyl chains) by elution of the column with a 10-60% propan-1-ol gradient over 20 mL. Fractions (1 mL) were collected, dried under nitrogen, and then subjected to methanolysis (50%) or strong acid hydrolysis (50%). For the latter, samples were dried in a glass capillary tube, and hydrolysed with 6 M hydrochloric acid at 110 °C for 16 hr under vacuum. The samples were dried under nitrogen, washed with toluene and methanol to remove residual acid and released *myo*-inositol TMS derivitized before TMS derivation prior to GC-MS analysis. Inositol was quantitated by selective ion monitoring (SIM) for ions at m/*z* 318-323.

Liquid chromatography-mass spectrometry (LC-MS) analysis. Total lipids were extracted from magnet-purified *P. falciparum*-infected RBC containing late trophozoite stages. Lipid extracts were suspended in 1-butanol/10 mM ammonium formate in methanol (1:1, 100 μL) and 5 μL aliquots injected onto a Ascentis Express RP Amide C18 + Amide column (50 mm × 2.1 mm × 2.7 μm Supelco) on an Agilent 1200 LC. Samples were eluted with a gradient of water/methanol/tetrahydrofuran (50:20:30, v/v) to water/methanol/tetrahydrofuran (5:20:75, v/v), at 0.2 $mLmin^{-1}$ over

5 min and the final buffer held for 3 min. Eluted material was analysed by electrospray ionisation-mass spectrometry (ESI-MS) using an Agilent QTOF 6520 (for full scans) and an Agilent Triple Quad 6410, for precursor ion and neutral loss scanning and multiple reaction monitoring (MRM), respectively. Samples were introduced using nanospray tips. Positive precursor ion scanning was used to identify molecular species of phosphatidylcholine (PC) (m/*z* 184.1), sphingomyelin (SM) (m/*z* 184.1), while negative precursor ion scanning was used to identify molecular species of PI (m/*z* 241) and phosphatidylglycerol (PG) (m/*z* 153). Neutral loss scanning was used to identify molecular species of phosphatidylethanolamine (PE) (m/*z* 141 in positive ion mode) and phosphatidylserine (PS) (m/*z* 87 in negative ion mode). Capillary and fragmentor voltages were 4.4–5.5 kV and 60–160 V, respectively. ESI-MS/MS spectra were recorded using collision voltages of 20–60 V. In all cases, the collision gas was nitrogen at 7 $Lmin^{-1}$. Data was analysed using MassHunter software (Agilent). Accurate mass full scans (MZmine): Capillary, fragmentor, and skimmer voltages were 4.5 kV, 100 V and 60 V, respectively and drying gas temperature was 325 °C. In all cases, the collision gas was nitrogen at 7 $Lmin^{-1}$. Profiling raw data obtained from Agilent QTOF were converted to mzdata format using Mass Hunter Qualitative software and imported to MZmine software version 2.4. Raw data was processed by mass detection with the noise level setting as 1×10^4 and chromatogram build with m/*z* tolerance at 0.01. Lipid species were identified according to the accurate mass and retention time.

Gene knock-out studies. A gene disruption construct was generated by insertion of a 5' (563bp) and 3' (529bp) segment of PF3D7_0511800 into pCC-1 (Maier *et al.*, 2008), with the restriction enzymes *Sac* II/*Spe* I and *Eco* RI/*Avr* II. The segments

were amplified from 3D7 genomic DNA using oligonucleotide primers Aw915/ Aw916 and Aw917/Aw918, respectively. Primer pair aw919/920 was used to amplify a targeting sequence for 3' replacement, which was inserted into the pHAST vector (*Sac* I/*Xho* I). Integration of the plasmid into the genome resulted in the expression of a 3xHA and Strep-tagged INO1 protein.

Oligonucleotides and DNA analysis: The following oligonucleotides were used:

Aw915: atcccgcgGTTCAAATATTAAGAGACTC

Aw916: gatactagTGGAGCATATGCATGTTCTTTATCC

Aw917: atcgaattcGATTGTTTAGTTCGTAACAAAGTTTTTG

Aw918: gatcctaggCCTGTTCCAAAGTAAAAGTCGAGGAGG

Aw919: atcccgcgGTGACTATGTACGTGCTAATG

Aw920: gatctcgagAATCATATATGGTAAATCAATATGAGC

Underlined are restriction sites introduced for cloning purposes. Genomic DNA was prepared with the DNeasy Tissue Kit (Qiagen) and subjected to Southern Blot analysis using the Roche DIG system following the manufacturer's instructions.

Acknowledgements

We thank Ms Monica Brown at the Walter and Eliza Hall Institute of Medical Research for technical assistance, Professor Andrew Holmes for providing authentic *myo*-inositol 3-phosphate, Dr Maria Doyle (Melbourne University) for discussions, and the Australian Red Cross Blood service (Melbourne), for provision of serum. This work was supported by program (APP406601) and project (APP1006024) grants and the Independent Research Institute Infrastructure Support Scheme from the National Health and Medical Research Council of Australia (NHMRC) and the Victorian State Government Operational Infrastructure Support scheme. JIM was

supported by a Royal Society Travelling Fellowship. MJM is an NHMRC Principal Research Fellow. AFC is an International Scholar of the Howard Hughes Medical Institute. AGM is an ARC Australian Research Fellow. None of the authors have a conflict of interest with the work reported in this study.

References

Allan, D. (1982) Inositol lipids and membrane function in erythrocytes. *Cell Calcium* **3**: 451-465.

Ben Mamoun, C., Prigge, S.T., and Vial, H. (2010) Targeting the lipid metabolic pathways for the treatment of malaria. *Drug Dev Res* **71**: 44-55.

Besteiro, S., Vo Duy, S., Perigaud, C., Lefebvre-Tournier, I., and Vial, H.J. (2010) Exploring metabolomic approaches to analyse phospholipid biosynthetic pathways in *Plasmodium*. *Parasitology* **137**: 1343-1356.

Bhattacharjee, S., Stahelin, R.V., and Haldar, K. (2012a) Host targeting of virulence determinants and phosphoinositides in blood stage malaria parasites. *Trends Parasitol* **28**: 555-562.

Bhattacharjee, S., Stahelin, R.V., Speicher, K.D., Speicher, D.W., and Haldar, K. (2012b) Endoplasmic reticulum PI(3)P lipid binding targets malaria proteins to the host cell. *Cell* **148**: 201-212.

Boddey, J.A., and Cowman, A.F. (2013) Plasmodium nesting: remaking the erythrocyte from the inside out. *Annu Rev Microbiol* .

Botté, C.Y., Yamaryo-Botté, Y., Rupasinghe, T.W.T., Mullin, K.A., MacRae, J.I., Spurck, T.P., *et al.* (2013) Atypical lipid composition in the purified relict plastid (apicoplast) of malaria parasites. *Proc Natl Acad Sci U S A* **110**: 7506-7511.

Bozdech, Z., Llinas, M., Pulliam, B.L., Wong, E.D., Zhu, J., and DeRisi, J.L. (2003) The transcriptome of the intraerythrocytic developmental cycle of *Plasmodium falciparum*. *PLoS Biol* **1**: E5.

Chang, T., Milne, K.G., Güther, M.L.S., Smith, T.K., and Ferguson, M.A.J. (2002) Cloning of *Trypanosoma brucei* and *Leishmania major* genes encoding the GlcNAc-phosphatidylinositol de-N-acetylase of glycosylphosphatidylinositol

biosynthesis that is essential to the African sleeping sickness parasite. *J Biol Chem* **277**: 50176-50182.

Chen, Y.-L., Kauffman, S., and Reynolds, T.B. (2008) *Candida albicans* uses multiple mechanisms to acquire the essential metabolite inositol during infection. *Infect Immun* **76**: 2793-2801.

Debierre-Grockiego, F., and Schwarz, R.T. (2010) Immunological reactions in response to apicomplexan glycosylphosphatidylinositols. *Glycobiology* **20**: 801-811.

Deranieh, R.M., He, Q., Caruso, J.A., and Greenberg, M.L. (2013) Phosphorylation regulates *myo*-inositol-3-phosphate synthase: A novel regulatory mechanism of inositol biosynthesis. *J Biol Chem* .

Di Daniel, E., Mok, M.H.S., Mead, E., Mutinelli, C., Zambello, E., Caberlotto, L.L., *et al.* (2009) Evaluation of expression and function of the H+/myo-inositol transporter HMIT. *BMC Cell Biol* **10**: 54.

Dondorp, A.M., Nosten, F., Yi, P., Das, D., Phyo, A.P., Tarning, J., *et al.* (2009) Artemisinin resistance in *Plasmodium falciparum* malaria. *N Engl J Med* **361**: 455-467.

Elabbadi, N., Ancelin, M.L., and Vial, H.J. (1994) Characterization of phosphatidylinositol synthase and evidence of a polyphosphoinositide cycle in *Plasmodium*-infected erythrocytes. *Mol Biochem Parasitol* **63**: 179-192.

Fischbach, A., Adelt, S., Müller, A., and Vogel, G. (2006) Disruption of inositol biosynthesis through targeted mutagenesis in *Dictyostelium discoideum*: generation and characterization of inositol-auxotrophic mutants. *Biochem J* **397**: 509-518.

Fischl, A.S., Homann, M.J., Poole, M.A., Carman, G.M. (1986) Phosphatidylinositol synthase from *Saccharomyces cerevisiae*. Reconstitution, characterization, and regulation of activity. *J. Biol. Chem*. **261**, 3178-3183

Gerold, P., Dieckmann-Schuppert, A., and Schwarz, R.T. (1994) Glycosylphosphatidylinositols synthesized by asexual erythrocytic stages of the malarial parasite, *Plasmodium falciparum*. Candidates for plasmodial glycosylphosphatidylinositol membrane anchor precursors and pathogenicity factors. *J Biol Chem* **269**: 2597-2606.

Gonzalez-Salgado, A., Steinmann, M.E., Greganova, E., Rauch, M., Mäser, P., Sigel, E., and Bütikofer, P. (2012) *myo*-Inositol uptake is essential for bulk inositol phospholipid but not glycosylphosphatidylinositol synthesis in *Trypanosoma brucei*. *J Biol Chem* **287**: 13313-13323.

Ilg, T. (2002) Generation of myo-inositol-auxotrophic *Leishmania mexicana* mutants by targeted replacement of the *myo*-inositol-1-phosphate synthase gene. *Mol. Biochem. Parasitol.* **120**: 151-156.

Irvine, R.F., and Schell, M.J. (2001) Back in the water: the return of the inositol phosphates. *Nat Rev Mol Cell Biol* **2**: 327-338.

Lambros, C., and Vanderberg, J.P. (1979) Synchronization of *Plasmodium falciparum* erythrocytic stages in culture. *J Parasitol* **65**: 418-420.

Lasonder, E., Green, J.L., Camarda, G., Talabani, H., Holder, A.A., Langsley, G., and Alano, P. (2012) The *Plasmodium falciparum* schizont phosphoproteome reveals extensive phosphatidylinositol and cAMP-protein kinase A signaling. *J Proteome Res* **11**: 5323-5337.

Le Roch, K.G., Zhou, Y., Blair, P.L., Grainger, M., Moch, J.K., Haynes, J.D., *et al.* (2003) Discovery of gene function by expression profiling of the malaria parasite life cycle. *Science* **301**: 1503-1508.

Luo, Y., Qin, G., Zhang, J., Liang, Y., Song, Y., Zhao, M., *et al.* (2011) D-*myo*-inositol-3-phosphate affects phosphatidylinositol-mediated endomembrane function in *Arabidopsis* and is essential for auxin-regulated embryogenesis. *Plant Cell* **23**: 1352-1372.

Macrae, J.I., Dixon, M.W., Dearnley, M.K., Chua, H.H., Chambers, J.M., Kenny, S., *et al.* (2013) Mitochondrial metabolism of sexual and asexual blood stages of the malaria parasite *Plasmodium falciparum*. *BMC Biol* **11**: 67.

Macrae, J.I., Sheiner, L., Nahid, A., Tonkin, C., Striepen, B., and McConville, M.J. (2012) Mitochondrial metabolism of glucose and glutamine is required for intracellular growth of *Toxoplasma gondii*. *Cell Host Microbe* **12**: 682-692.

Maier, A.G., Rug, M., O'Neill, M.T., Brown, M., Chakravorty, S., Szestak, T., *et al.* (2008) Exported proteins required for virulence and rigidity of *Plasmodium falciparum*-infected human erythrocytes. *Cell* **134**: 48-61.

Majumder, A.L., Chatterjee, A., Ghosh Dastidar, K., and Majee, M. (2003) Diversification and evolution of L-*myo*-inositol 1-phosphate synthase. *FEBS Lett* **553**: 3-10.

Mantel, P.-Y., Hoang, A.N., Goldowitz, I., Potashnikova, D., Hamza, B., Vorobjev, I., *et al.* (2013) Malaria-infected erythrocyte-derived microvesicles mediate cellular Communication within the parasite population and with the host immune system. *Cell Host Microbe* **13**: 521-534.

Martin, K.L., and Smith, T.K. (2006a) The glycosylphosphatidylinositol (GPI) biosynthetic pathway of bloodstream-form *Trypanosoma brucei* is dependent on the *de novo* synthesis of inositol. *Mol Microbiol* **61**: 89-105.

Martin, K.L., and Smith, T.K. (2006b) Phosphatidylinositol synthesis is essential in bloodstream form *Trypanosoma brucei*. *Biochem J* **396**: 287-295.

McConville, M.J., and Blackwell, J.M. (1991) Developmental changes in the glycosylated phosphatidylinositols of *Leishmania donovani*. Characterization of the promastigote and amastigote glycolipids. *J Biol Chem* **266**: 15170-15179.

McConville, M.J., Homans, S.W., Thomas-Oates, J.E., Dell, A., and Bacic, A. (1990) Structures of the glycoinositolphospholipids from *Leishmania major*. A family of novel galactofuranose-containing glycolipids. *J. Biol. Chem.* **265**: 7385-7394.

Michell, R.H. (2008) Inositol derivatives: evolution and functions. *Nat Rev Mol Cell Biol* **9**: 151-161.

Miller, D.J., and Allemann, R.K. (2007) *myo*-Inositol monophosphatase: a challenging target for mood stabilising drugs. *Mini Rev Med Chem* **7**: 107-113.

Miller LH, Ackerman HC, Su XZ, Wellems TE (2013) Malaria biology and disease pathogenesis: insights for new treatments. Nat Med 19: 156-167.

Naik, R.S., Branch, O.H., Woods, A.S., Vijaykumar, M., Perkins, D.J., Nahlen, B.L., *et al.* (2000) Glycosylphosphatidylinositol anchors of *Plasmodium falciparum*: molecular characterization and naturally elicited antibody response that may provide immunity to malaria pathogenesis. *J Exp Med* **192**: 1563-1576.

Olszewski, K.L., Morrisey, J.M., Wilinski, D., Burns, J.M., Vaidya, A.B., Rabinowitz, J.D., and Llinás, M. (2009) Host-parasite interactions revealed by *Plasmodium falciparum* metabolomics. *Cell Host Microbe* **5**: 191-199.

Regev-Rudzki, N., Wilson, D.W., Carvalho, T.G., Sisquella, X., Coleman, B.M., Rug, M., *et al.* (2013) Cell-cell communication between malaria-infected red blood cells via exosome-like vesicles. *Cell* **153**: 1120-1133.

Reynolds, T.B. (2009) Strategies for acquiring the phospholipid metabolite inositol in pathogenic bacteria, fungi and protozoa: making it and taking it. *Microbiology* **155**: 1386-1396.

Rommisch, K. (2012) Diversion at the ER: How *Plasmodium falciparum* exports proteins into host erythrocytes. *F1000Research* **1**.

Sana, T.R., Gordon, D.B., Fischer, S.M., Tichy, S.E., Kitagawa, N., Lai, C., *et al.* (2013) Global mass spectrometry based metabolomics profiling of erythrocytes infected with *Plasmodium falciparum*. *PLoS One* **8**: e60840.

Sanders, P.R., Gilson, P.R., Cantin, G.T., Greenbaum, D.C., Nebl, T., Carucci, D.J., *et al.* (2005) Distinct protein classes including novel merozoite surface antigens in raft-like membranes of *Plasmodium falciparum*. *J Biol Chem* **280**: 40169-40176.

Saunders, E.C., Ng, W.W., Chamber, J.M., Ng, M., Naderer, T., Kroemer, J.O., *et al.* (2011) Isoptopomer profiling of *Leishmania mexicana* promastigotes reveals important roles for succinate fermentation and aspartate uptake in TCA cycle anaplerosis, glutamate synthesis and growth. *J Biol Chem* **286**: 27706-27717.

Shi, J., Wang, H., Hazebroek, J., Ertl, D.S., and Harp, T. (2005) The maize low-phytic acid 3 encodes a myo-inositol kinase that plays a role in phytic acid biosynthesis in developing seeds. *Plant J* **42**: 708-719.

Stephens, L.R., Kay, R.R., and Irvine, R.F. (1990) A *myo*-inositol D-3 hydroxykinase activity in *Dictyostelium*. *Biochem J* **272**: 201-210.

Stritzke, C., Nalaskowski, M.M., Fanick, W., Lin, H., and Mayr, G.W. (2012) A *Plasmodium* multi-domain protein possesses multiple inositol phosphate kinase activities. *Mol Biochem Parasitol* **186**: 134-138.

Tarun, A.S., Vaughan, A.M., and Kappe, S.H. (2009) Redefining the role of *de novo* fatty acid synthesis in *Plasmodium parasites*. *Trends Parasitol* **25**: 545-550.

Tawk, L., Chicanne, G., Dubremetz, J.-F., Richard, V., Payrastre, B., Vial, H.J., *et al.* (2010) Phosphatidylinositol 3-phosphate, an essential lipid in *Plasmodium*, localizes to the food vacuole membrane and the apicoplast. *Eukaryot Cell* **9**: 1519-1530.

Tawk, L., Dubremetz, J.-F., Montcourrier, P., Chicanne, G., Merezegue, F., Richard, V., *et al.* (2011) Phosphatidylinositol 3-monophosphate is involved in toxoplasma apicoplast biogenesis. *PLoS Pathog* **7**: e1001286.

Teng, R., Junankar, P.R., Bubb, W.A., Rae, C., Mercier, P., and Kirk, K. (2009) Metabolite profiling of the intraerythrocytic malaria parasite *Plasmodium falciparum* by (1)H NMR spectroscopy. *NMR Biomed* **22**: 292-302.

Trager, W., and Jensen, J.B. (1976) Human malaria parasites in continuous culture. *Science* **193**: 673-675.

Trang, D.T.X., Huy, N.T., Kariu, T., Tajima, K., and Kamei, K. (2004) One-step concentration of malarial parasite-infected red blood cells and removal of contaminating white blood cells. *Malar J* **3**: 7.

Vadnal, R.E., Parthasarathy, R., Parthasarathy, L., Ramesh, T.G., and Shyamaladevi, C.S. (1992) The identification of a membrane-bound *myo*-inositol 1-phosphatase in rat brain, liver, and testes. *Biochem Int* **26**: 935-941.

Wang, Y., Liu, T.-B., Delmas, G., Park, S., Perlin, D., and Xue, C. (2011) Two major inositol transporters and their role in cryptococcal virulence. *Eukaryot Cell* **10**: 618-628.

Wengelnik, K., and Vial, H.J. (2007) Characterisation of the phosphatidylinositol synthase gene of *Plasmodium* species. *Res Microbiol* **158**: 51-59.

WHO (2013) Malaria (Fact Sheet) No94. World Health Organization.

Xue, C., Liu, T., Chen, L., Li, W., Liu, I., Kronstad, J.W., *et al.* (2010) Role of an expanded inositol transporter repertoire in *Cryptococcus neoformans* sexual reproduction and virulence. *MBio* **1**.

Figure Legends

Figure 1. Multivariate analysis of *P. falciparum*-infected RBC cultures.

(A) Polar metabolites were extracted from synchronized *P. falciparum* 3D7 RBC cultures (8% parasitaemia) enriched for ring (ring-iRBC), trophozoite (troph-iRBC), and schizont (schiz-iRBC) stages and analyzed by GC/MS. Principal Component Analysis (PCA) of the data matrix generated by progressive clustering and deconvolution of GC-MS chromatograms. The X and Y axes represent the principal components accounting for the greatest (29.8%) and second greatest (22.4%) variability, respectively. (B) Polar metabolites were extracted from infected and uninfected RBCs (iRBC/uRBC) obtained from trophozoite (troph) and schizont (schiz) enriched synchronized cultures. The X and Y axes of the PCA plots represent the principal components accounting for 30.1% and 21.0% variability, respectively. (C and D). Targeted Z-score plots of selected metabolites in trophozoite- (C) and schizont- (D) iRBCs. Plotted z-scores show the mean and standard deviations of individual metabolites in 8 replicate analyses normalized to the appropriate uRBC

sample set (also 8 replicates). Filled grey circles refer to metabolite levels in uRBCs (which typically cluster within 5 standard deviations of the mean) while filled blue circles show metabolite levels in trophozoite- and schizont-infected RBCs (as s.d. from the mean of uRBC). Metabolite levels that deviate from the mean by >5 s.d. are considered significant. Note that the z-score plots are truncated at 25 s.d. for clarity.

Figure 2. Inositol metabolite levels in infected and uninfected RBC.

Polar metabolites were isolated from synchronized *P. falciparum* cultures (8% parasitaemia) containing unfractionated ring-infected RBC (Ring), magnet-purified trophozoite-RBC (Troph) or schizont-RBC (Schiz) stages, uninfected RBC (uRBC, purified from the schizont-infected culture), and RBCs that had never been exposed to parasites (nRBC). Intracellular pool sizes of *myo*-inositol (*myo*-Ino) and inositol 3-phosphate (Ino3P) in 10^8 cell equivalents were determined by GC-MS. In the box-whisker plots, thick horizontal lines indicate the median abundance, boxes the interquartile range, whiskers extreme non-outliers, and circles outliers. n = 5-8.

Figure 3. Biosynthesis of inositol metabolites *in vivo*.

(A) *De novo* biosynthetic pathway of *myo*-inositol. The conversion of glucose 6-phosphate (Glc6P) to inositol 3-phosphate (Ino3P) and *myo*-inositol (*myo*-Ino) is catalyzed by inositol 3-phosphate synthase (INO1) and inositol monophosphatase (IMPase), respectively.

(B) Synchronized *P. falciparum* RBC cultures (8% parasitaemia) were pulse-labelled with ^{13}C-glucose stages for 2 hr at different stages of development. Enrichment of ^{13}C in Glc6P (black bars), Ino3P (grey bars), and *myo*-inositol (white bars) (relative to exogenous glucose) in unfractionated ring-infected RBCs (Ring) and purified

trophozoite- (Troph) and schizont-infected (Schiz) RBCs was determined by GC-MS. *n* = 5-8. Data for uRBCs and nRBCs is shown in Table S1.

(C) Levels of INO1 activity in synchronized *P. falciparum* RBC cultures. Cell lysates (5 x 10^6 cell equivalents) were incubated with ^{13}C-Glc6P and synthesis of ^{13}C-Ino3P determined by GC-MS. Ino3P synthesis is shown as pmol/min, and is based on initial rate kinetics in a time course experiment. Negligible activity was detected in RBCs that had never been exposed to parasites (nRBC). *n* = 4 and error bars indicate standard deviation.

(D) Synchronized *P. falciparum* RBC cultures containing trophozoite stages were labelled with ^{13}C-glucose with or without supplementation of the medium with 4 mM *myo*-inositol. The abundance and ^{13}C-enrichment in Ino3P and *myo*-inositol was determined by GC-MS. *n* = 4 and error bars indicate standard deviation.

Figure 4. Stage-specific changes in PI synthesis

(A) Synchronized *P. falciparum* RBC cultures were harvested at different stages of the 48 hr cycle and total PI levels determined by analysis of inositol content in the organic (lipid) phase. Abbreviations as above. *n* = 4-6 and error bars indicate standard deviation.

(B) Synchronized *P. falciparum*-infected RBC cultures were labelled with ^{13}C-glucose for 16 hr and total lipids analysed by LC-MS. Precursor scanning for m/z 241 or m/z 247 was used to quantitate relative abundance of PI molecular species containing an unlabelled and $^{13}C_6$-inositol head-groups, respectively. Selected species (i.e. C34:1 and C36:1 are indicated). The chromatograms are representative of 4 separate experiments.

(C) Abundance of all PI species and relative abundance of ^{13}C-PI species following growth in the presence or absence of 4 mM exogenous *myo*-inositol. $n = 4$ and error bars indicate standard deviation.

Figure 5. Endogenous Ino3P, and not exogenous *myo*-inositol is incorporated into GPI glycolipids

(A) *P. falciparum*-infected RBCs were metabolically labelled with ^{3}H-GlcN or ^{3}H-*myo*-inositol for 24 hr and labelled inositol (glyco)lipids resolved by HPTLC. Equivalent cell equivalents (1.25×10^{7}) were treated with PI-PLC, GPI-PLD or a buffer control prior to HPTLC analysis. Labelled glycolipid species were detected by fluorography, and assigned the following structures based on previous studies {Gerold 1994}: glucosamine-acyl-PI (GlcN-acyl-PI), glucosamine-acyl-PI (GlcN-PI), mannose$_4$-glucosamine-acyl-PI (Man$_4$GlcN-acyl-PI), ethanolaminephosphate-mannose$_4$-glucosamine-acyl-PI (EtNP-Man$_4$GlcN-acyl-PI), and PI. A band with a slower HPTLC mobility was generated following GPI-PLD treatment of the ^{3}H-inositol labelled lipids. This species was has the expected HPTLC mobility of lyso-PI and may have been generated by other lipases in the serum.

(B) *P. falciparum* infected RBCs were labelled with 13 mM ^{13}C-glucose (2 hr post-synchronisation) and harvested when parasites reached late trophozoite-stage (28 hr). A total lipid extract was subjected to hydrophobic interaction chromatography to resolve PI species (two acyl chains) from GPI glycolipids (three acyl chains). Enrichment of ^{13}C into the mannose and inositol moieties of the GPI fraction were determined by GC-MS after strong aqueous (6 M HCl, 100 °C, 24 hr) and methanolysis (0.5 methanolic-HCl, 80 °C, 24 hr), respectively. Error bars indicate standard deviation ($n = 4$).

Figure 6. Targeted replacement of *P. falciparum INO1*

(A) Schematic representation showing the targeted replacement of the *INO1* gene (PF3D7_0511800) in the wild-type cells with a non-functional copy (hDHFR) from a plasmid and the resulting disrupted locus. Restriction sites for *Age* I (A), *Eco* RV (E), *Kpn* I (K), and *Xba* I (X) are indicated, along with the expected fragment sizes following double-digestion.

(B) Southern blot of the wild-type and *INO1* mutant cell lines. DNA from wild-type (3D7) and mutant cells (3D7Δ PF3D7_0511800) were digested with *Age* I/*Kpn* I or *Eco* RV/*Xba* I and probed as indicated. Similar results were obtained when the same gene was disrupted in the CS2 strain was attempted (results not shown).

(C) Schematic representation showing the targeted insertion of a 3×HA/Strep tag onto the 3'-end of the *INO1* gene in wild-type cells from a plasmid and the resulting disrupted locus. (D) A Western blot using biotin (anti-streptavidin antibodies) indicated expression of the HA/STREP-tagged copy of INO1 in the mutant cell line. PfHSP70 is shown as a loading control.

Figure 7. Hypothetical model for metabolic compartmentalization of PI biosynthesis in *P. falciparum*. *P. falciparum* trophozoite and schizont stages up-regulate *myo*-inositol synthesis, via Ino3P, for bulk membrane PI and GPI glycolipid biosynthesis. These stages can also scavenge exogenous *myo*-inositol from the host, although exogenous *myo*-inositol is only used to synthesize bulk PI. A similar metabolic compartmentalization of inositol metabolism and PI synthesis occurs in African trypanosomes (Gonzalez-Salgado *et al.*, 2012; Martin and Smith, 2006a). Metabolic compartmentalization in these parasites may be achieved by the

sequestration of single/multiple isoforms of PI-synthase to the lumen of the ER and Golgi and single/multiple isoforms of IMPase to the cytoplasmic leaflet of the ER in conjunction with an, as yet to be identified, *myo*-inositol transporter. Multiple transporters are required for the transport of glucose and *myo*-inositol across the RBC plasma membrane (RBC-PM), parasitophorous vacuolar membrane (PVM), and parasite plasma membrane (*Pf* PM).

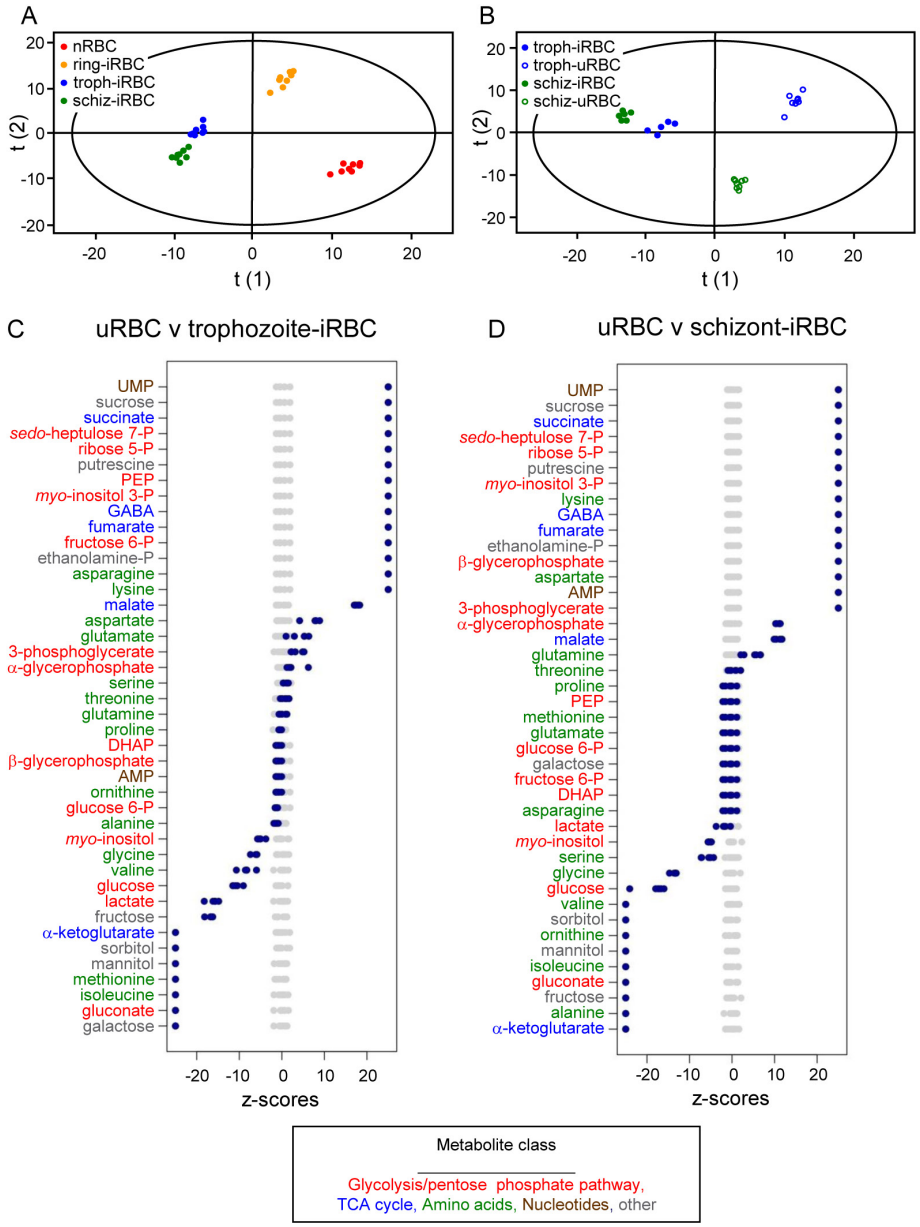

mmi_12496_f1.tif

mmi_12496_f2.tif

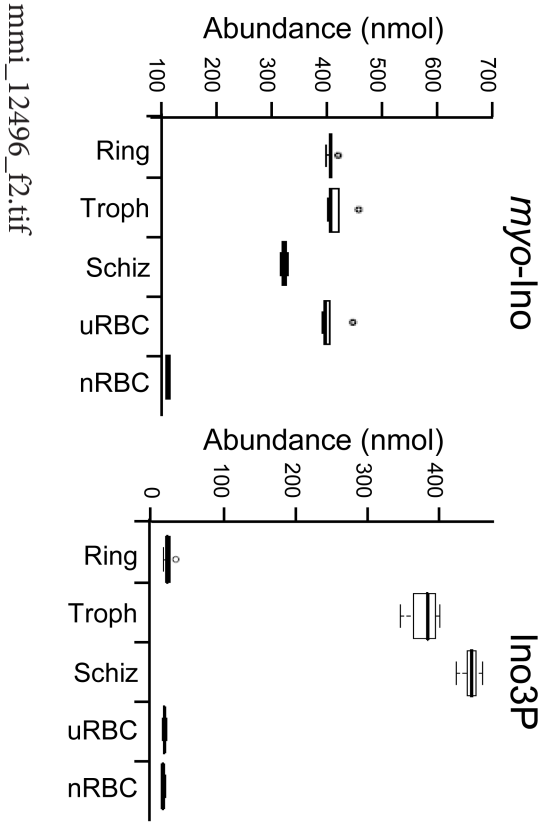

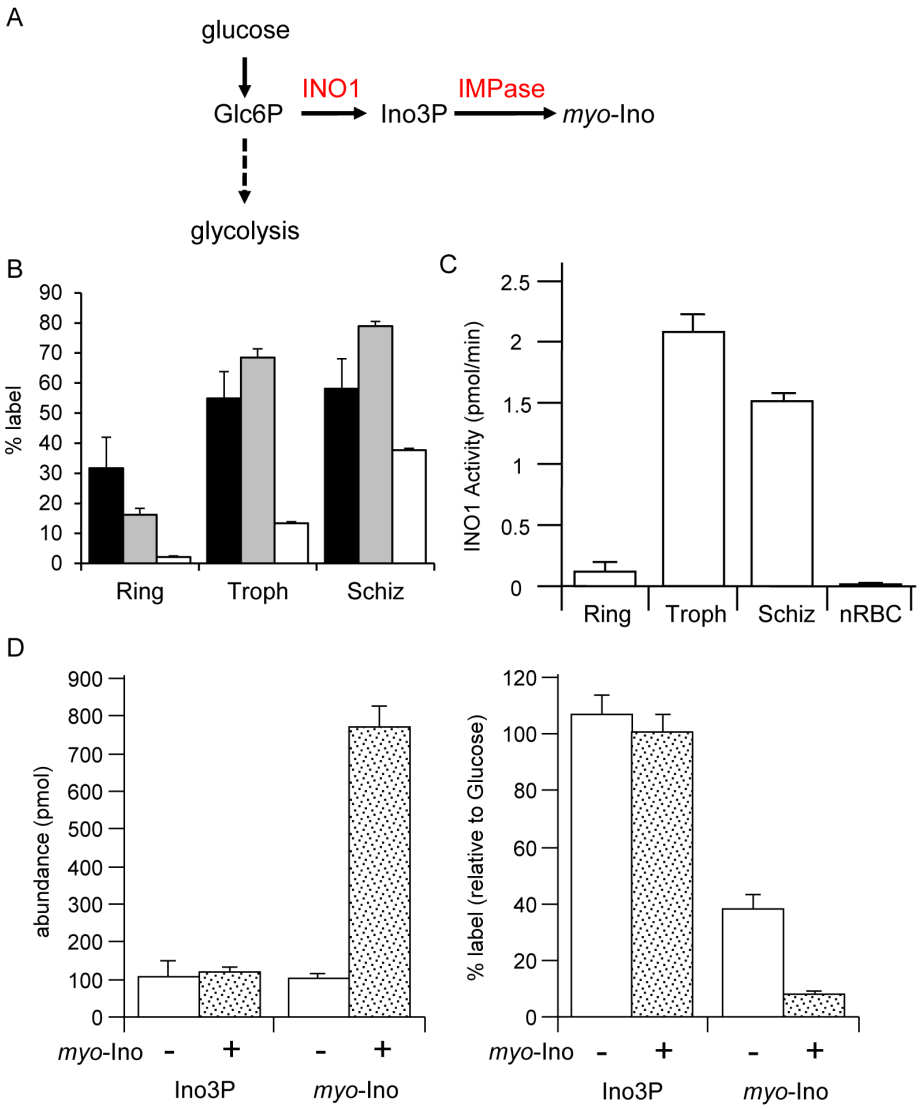

mmi_12496_f3.tif

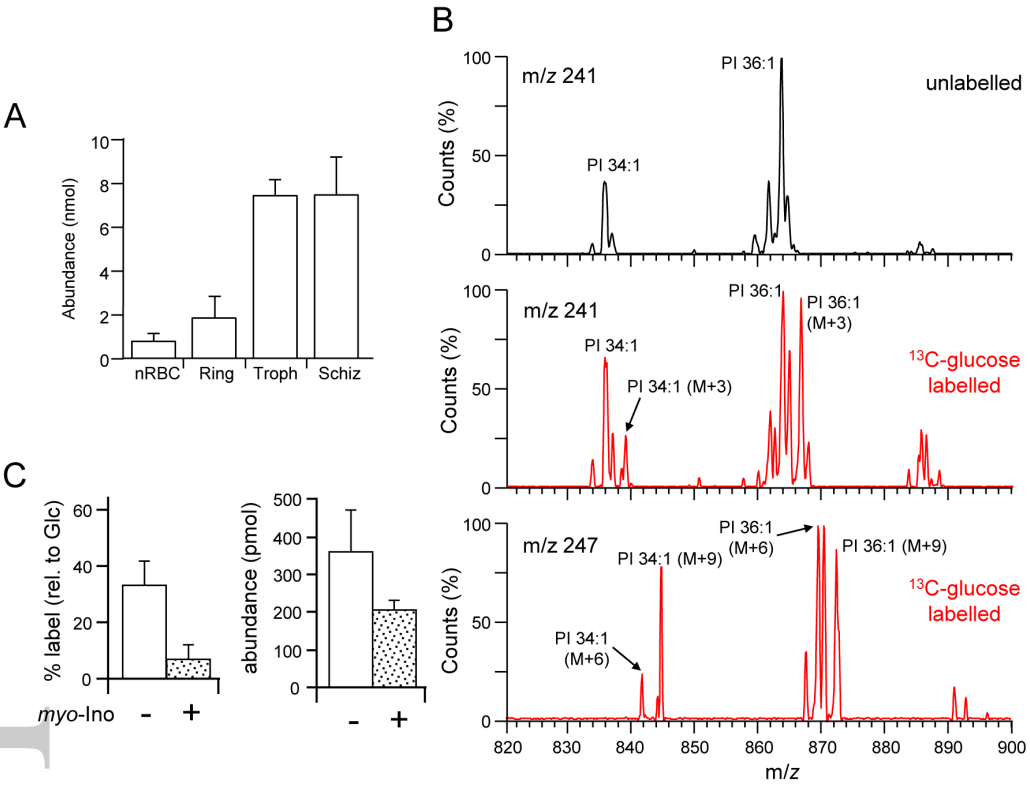

mmi_12496_f4.tif

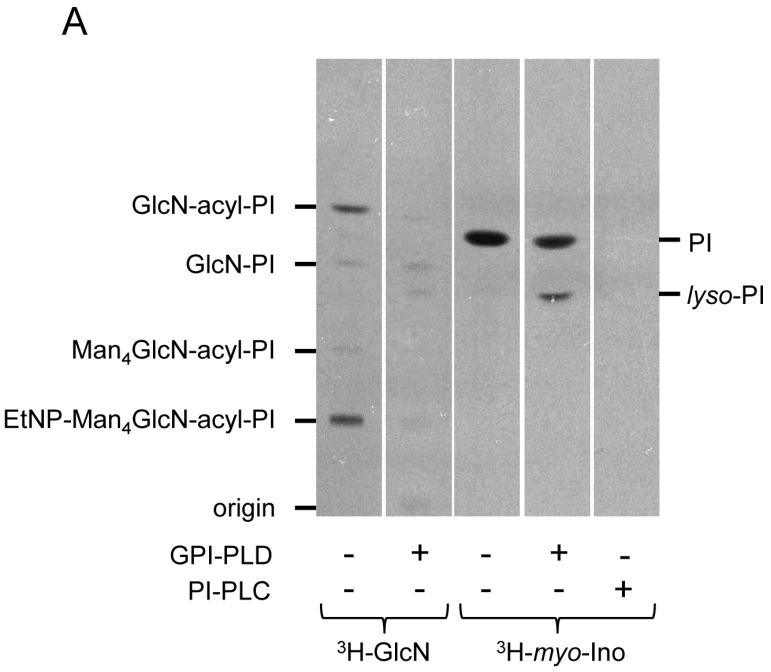

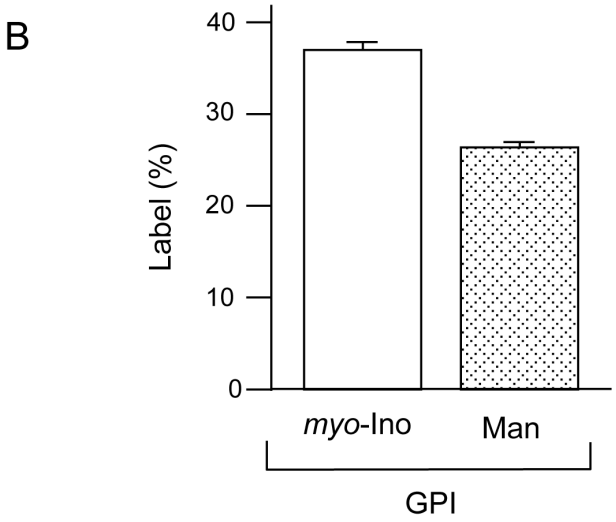

mmi_12496_f5.tif

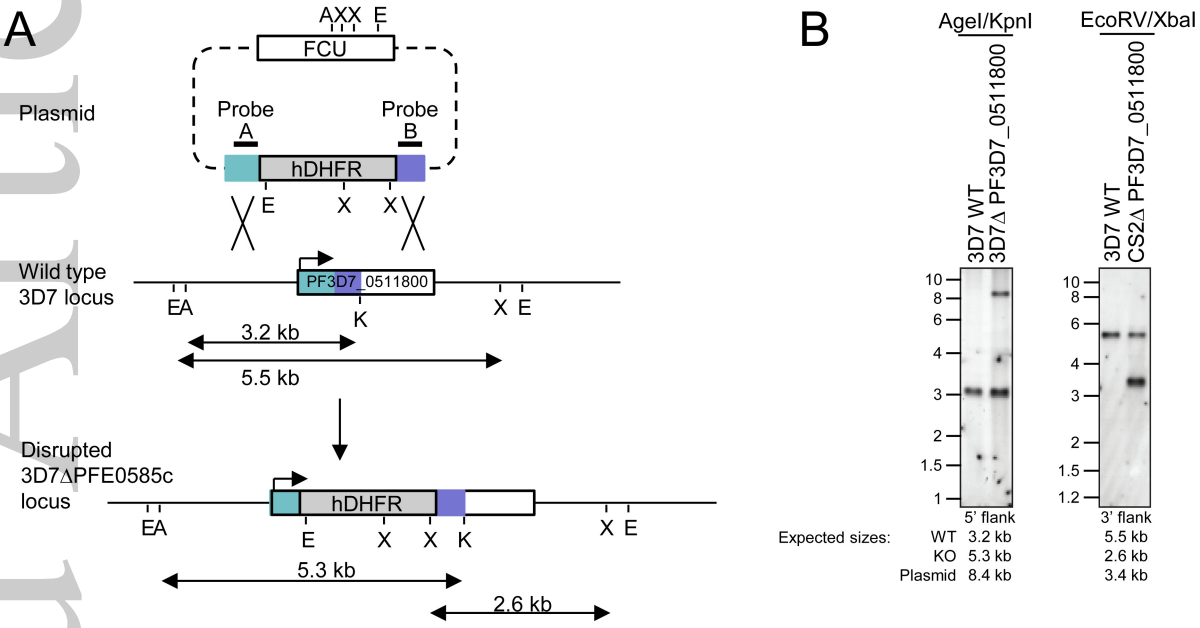

mmi_12496_f6.tif

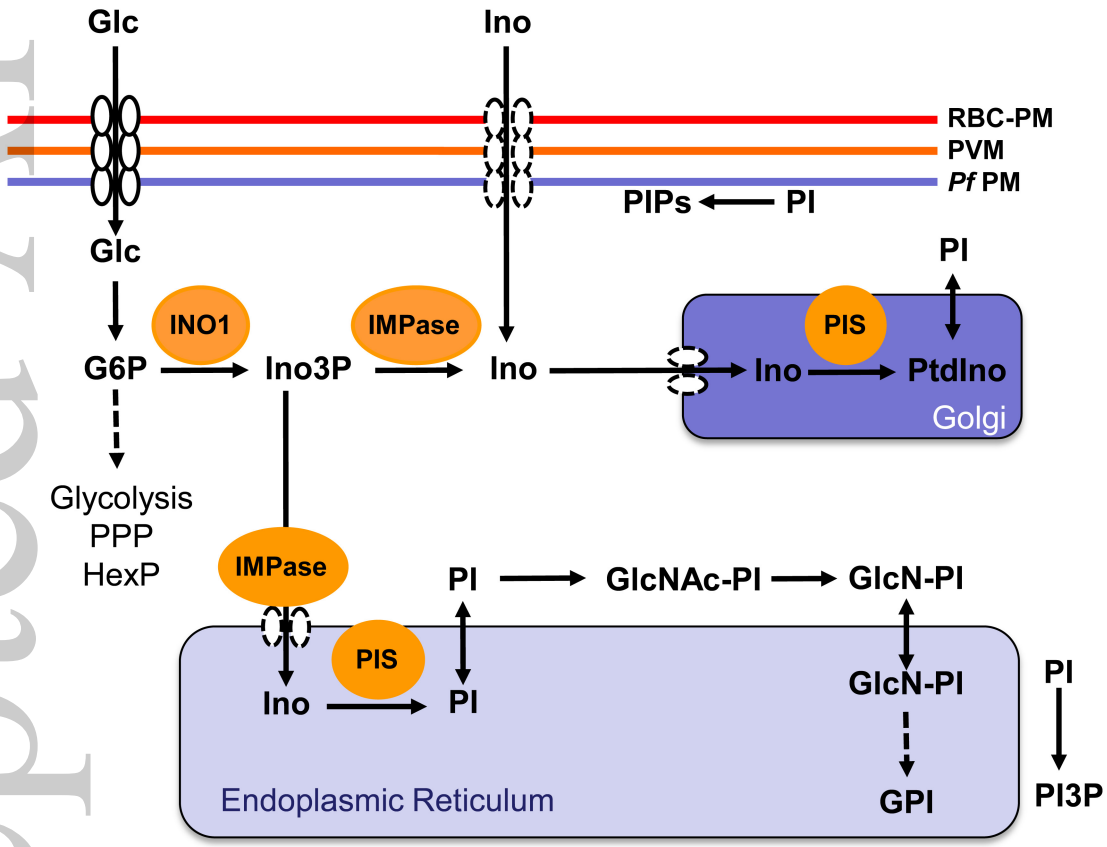

mmi_12496_f7.tif

Author/s:
MacRae, JI; Lopaticki, S; Maier, AG; Rupasinghe, T; Nahid, A; Cowman, AF; McConville, MJ

Title:
Plasmodium falciparum is dependent on de novo myo-inositol biosynthesis for assembly of GPI glycolipids and infectivity

Date:
2014-02-01

Citation:
MacRae, JI; Lopaticki, S; Maier, AG; Rupasinghe, T; Nahid, A; Cowman, AF; McConville, MJ, Plasmodium falciparum is dependent on de novo myo-inositol biosynthesis for assembly of GPI glycolipids and infectivity, MOLECULAR MICROBIOLOGY, 2014, 91 (4), pp. 762 - 776

Publication Status:
Accepted manuscript